Circulating CD138 enhances disease progression by augmenting autoreactive antibody production in a mouse model of systemic lupus erythematosus

Received for publication, May 10, 2021, and in revised form, July 29, 2021 Published, Papers in Press, August 6, 2021,
https://doi.org/10.1016/j.jbc.2021.101053

Lunhua Liu and Mustafa Akkoyunlu*

From the Laboratory of Bacterial Polysaccharides, Division of Bacterial Parasitic and Allergenic Products, Center for Biologics, Evaluation and Research, The US Food and Drug Administration, Silver Spring, Maryland, USA

Edited by Peter Cresswell

Systemic lupus erythematosus (SLE) is a progressive autoimmune disease characterized by high levels of antibodies directed against nuclear antigens. Elevated serum CD138, a heparan sulfate–bearing proteoglycan, correlates with increased disease activity in patients with SLE, but the contribution of CD138 to lupus disease is not known. Corroborating patient data, we detected an increase in serum CD138 in MRL/MpJ-Fas^{lpr}/J (MRL/Lpr) mice (a model for SLE disease) parallel to disease activity. Although T-cell receptor β (TCRβ)+CD138+ T cells typically expand in MRL/Lpr mice as the disease progresses, surprisingly, TCRβ+CD138− cells were the primary source of circulating CD138, as the transfer of TCRβ+CD138− cells, but not TCRβ+CD138+ cells, to young MRL/Lpr mice resulted in higher serum CD138 in the recipients. We found that trypsin was able to cleave CD138 from TCRβ+CD138+ cells, and that trypsin was highly expressed in TCRβ+CD138− cells. Moreover, trypsin inhibitors, the "defined trypsin inhibitor" and leupeptin, increased CD138 expression on TCRβ+CD138− cells, suggesting a contribution of cleaved CD138 to the increase in blood CD138 levels. Furthermore, soluble CD138 was able to bind "a proliferation-inducing ligand" (APRIL) and enhance APRIL-mediated plasma cell generation and autoreactive antibody production through the phosphorylation of extracellular signal–regulated kinase in B cells. The APRIL receptor "transmembrane activator, calcium modulator, and cyclophilin ligand interactor" was involved in the enhancement of APRIL activity by CD138, as the synergistic effect of APRIL and CD138 was ablated in transmembrane activator, calcium modulator, and cyclophilin ligand interactor–deficient B cells. These findings indicate a regulatory role for soluble CD138 in B-cell differentiation and autoreactive antibody production in SLE disease.

Systemic lupus erythematosus (SLE) is a chronic autoimmune disease characterized by hyperproduction of autoreactive antibodies that cause inflammation and multiple organ damage (1). This systemic pathological immune response, which involves both innate and adaptive immune system, is characterized by the elevation of multiple cytokines in serum. Increased serum levels of "A proliferation-inducing ligand" (APRIL), "B-cell–activating factor" (BAFF), interferon α, interferon γ, interleukin 6 (IL-6), IL-12, IL-17, and tumor necrosis factor alpha are found to be positively correlated with autoreactive antibody production, SLE Disease Activity Index scores, and organ involvement (2). Among these cytokines, APRIL and BAFF bind to B-cell maturation antigen (BCMA) and transmembrane activator, calcium modulator, cyclophilin ligand interactor (TACI), and BAFF in addition binds to BAFF receptor (3). Engagement of these three receptors can directly lead to the maturation, proliferation, and survival of B cells in addition to the formation of long-lived antibody-secreting plasma cells (3). Thus, considerable interest has been expressed in the development of APRIL and BAFF antagonists as therapeutic agents. A fully humanized anti-BAFF monoclonal antibody (belimumab), which effectively reduces disease activity and flare severity, has been approved in the United States and around the world for the treatment of lupus (4).

In addition to the increase in inflammatory cytokines, patients with SLE, but not patients with rheumatoid arthritis, manifest with elevated serum levels of CD138 (syndecan-1) (5, 6). As a member of the syndecan family of type I transmembrane proteoglycans, CD138 is composed of a core protein modified by heparan sulphate and chondroitin sulphate chains (7, 8). Membrane-bound CD138 has been shown to play an important role in wound healing, cell adhesion, and endocytosis (9). Its biological activity is mediated by the binding of its covalently attached glycosaminoglycan chains to several extracellular adhesion molecules, growth factors, cytokines, and chemokines (7, 10). The attachment of CD138 to these molecules results in the modification of their biological activity (7, 10).

Like the other three members of syndecan family molecules, the intact ectodomain of CD138 is constitutively shed from cells and forms soluble CD138 as part of normal cell surface heparan sulfate proteoglycan turnover (11, 12). In response to injury or infection, the ectodomain of CD138 is proteolytically shed from the cell surface by matrix metalloproteinases (MMPs), such as MMP9 and matrilysin

* For correspondence: Mustafa Akkoyunlu, Mustafa.Akkoyunlu@fda.hhs.gov.

(MMP7) (11, 13). Elevated soluble CD138 also regulates a variety of pathways that are related to wound healing, cell proliferation, and apoptosis (14). Excessive soluble CD138 has been shown to delay skin wound repair as it enhances elastase activity and inhibits growth factor action (15). Soluble CD138 is also involved in host response to tumor development. For example, soluble CD138 inhibits the mitogenicity of fibroblast growth factor 2 on B stem–like F32 cells, and overexpression of soluble ectodomain or the addition of exogenous CD138 ectodomain significantly inhibits the proliferation of MCF-7 breast cancer cell line (16, 17). Moreover, the impact of shed CD138 extends beyond cell to cell contact within the tumor microenvironment as the accumulation of soluble CD138 enhances the growth of myeloma tumors *in vivo* and promotes endothelial invasion and angiogenesis (18–20). Besides, in patients with myeloma and lung cancer, high levels of serum CD138 correlates with poor disease prognosis and survival (21, 22).

In patients with SLE, serum CD138 levels positively correlate with SLE Disease Activity Index and anti-dsDNA antibody levels (5, 6). But the origin and function of circulating CD138 in patients with lupus remain largely unknown. In this study, we investigated the origin and biological function of soluble CD138 in lupus development. We first focused on TCRβ+CD138+ cells as the source of soluble CD138 because we have recently reported the expansion of CD138 bearing TCRβ+ cells in various organs of the lupus prone MRL/MpJ-Fas^{lpr}/J (MRL/Lpr) mouse (23). Surprisingly, we found that activated TCRβ+CD138– cells produce more soluble CD138 than activated TCRβ+CD138+ cells. Moreover, the transfer of TCRβ+CD138– cells into MRL/Lpr mice led to higher serum CD138 measurement than the transfer of TCRβ+CD138+ cells did. In support of TCRβ+CD138– cells as the source of circulating CD138, we found higher expression of trypsin by TCRβ+CD138– cells than TCRβ+CD138+ cells, which effectively cleaved CD138 to produce its soluble form. Interestingly, we also found that binding of soluble CD138 to APRIL strongly enhanced APRIL-induced extracellular signal–regulated kinase (ERK) phosphorylation in B cells and promoted B-cell differentiation into antibody-secreting plasma cells.

Results

Activated TCRβ+CD138– cells release more soluble CD138 than TCRβ+CD138+ cells do

Patients with SLE manifest with increased serum CD138 levels, which correlate with disease activity and severity of nephritis (5, 6). By using the widely studied lupus prone MRL/Lpr mice, we investigated the source of CD138 in lupus disease (24). In MRL/Lpr mice, a single mutation in the *fas* apoptosis gene results in lymphoproliferation and autoreactive B- and T-cell activation (25). As a result, MRL/Lpr mice begin to manifest lupus symptoms such as anti-dsDNA antibodies and kidney dysfunction starting from 4 to 6 weeks of age, and the disease progresses with age (Fig. S1*A*) (25, 26). Analysis of serum CD138 in MRL/Lpr mice from different ages indicated that its levels increase with age (Fig. 1*A*). Thus, as reported in patients with lupus, serum CD138 levels positively correlate with the disease progression in MRL/Lpr mice. We have recently reported the expansion of TCRβ+CD138+ cells in MRL/Lpr mice (23). Spleens of 14-week-old MRL/Lpr mice harbor CD138-expressing plasmablasts, plasma cells, and TCRβ+CD138+ cells (Fig. 1*B* and Fig. S1*B*). As the disease progresses, both the CD138-expressing plasma cells and TCRβ+CD138+ T cells expand in the blood also (Fig. 1*C*). Importantly, the numbers and percentages of TCRβ+CD138+ cells were significantly higher than the plasma cells in both the spleen and the blood (Fig. 1, *B* and *C*). Thus, we speculated that the shedding of CD138 from TCRβ+CD138+ cells may be responsible for the elevated circulating CD138. To test this hypothesis, we adoptively transferred TCRβ+CD138+ or TCRβ+CD138– cells from 12- to 14-week-old MRL/Lpr mice into 8-week-old MRL/Lpr mice and measured serum CD138 levels in the recipient mice. Surprisingly, analysis of serum CD138 levels 3 days after the transfer indicated that the TCRβ+CD138– cell-transferred group had higher serum CD138 levels than PBS and TCRβ+CD138+ cell-transferred groups (Fig. 1*D*). Corroborating the adoptive transfer experiment results, when stimulated with anti-CD3 and anti-CD28 antibodies (αCD3/CD28), purified TCRβ+CD138– secreted more CD138 than activated TCRβ+CD138+ cells did (Fig. 1*E*). These data suggested that TCRβ+CD138– cells may be an important source of circulating CD138 in MRL/Lpr mice.

We have previously shown that most TCRβ+CD138+ cells are CD44+CD62L+ central memory T (TCM) cells, whereas TCRβ+CD138– cells consist of CD44-CD62L+ naive T (TN), CD44+CD62L– effector memory T (TEM) and TCM cells (23). When stimulated with αCD3/CD28, a slight increase in TN population was observed in TCRβ+CD138– cells after 48 and 72 h (Fig. S1*C*). There was no significant change in TCM and TEM frequency in stimulated TCRβ+CD138– cells (Fig. 1*F* and Fig. S1*C*). Stimulation also did not change the TCM and TEM population in TCRβ+CD138+ cells, although there was a slight decrease in TN population (Fig. 1*F* and Fig. S1*C*). Thus, activation does not meaningfully alter the memory phenotype of TCRβ+CD138+ and TCRβ+CD138– cells.

CD138 is cleaved from lupus T cells by trypsin

Next, we sought to determine how membrane-bound CD138 was released from lupus T cells. In a variety of cells ranging from epithelial cells, macrophages, and CD4+ T cells to cells from tumors, such as myeloma, pancreatic cancer, and melanoma, membrane CD138 is cleaved by different proteinases, such as MMP9, MT1-MMP, MT3-MMP, collagenase, and trypsin (11, 13, 19, 27–30). We therefore tested the activity of these proteinases on the cleavage of CD138 from lupus mouse T cells. We found that MMP9 was unable to cleave CD138 from TCRβ+CD138+ cells (Fig. 2*A* and Fig. S2, *A* and *B*). Similarly, collagenase I and D failed to shed CD138 from purified TCRβ+CD138+ cells (Fig. 2*B* and Fig. S2*C*). In contrast to MMP9 and collagenases I and D, we found that CD138 was highly sensitive to trypsin cleavage as after a

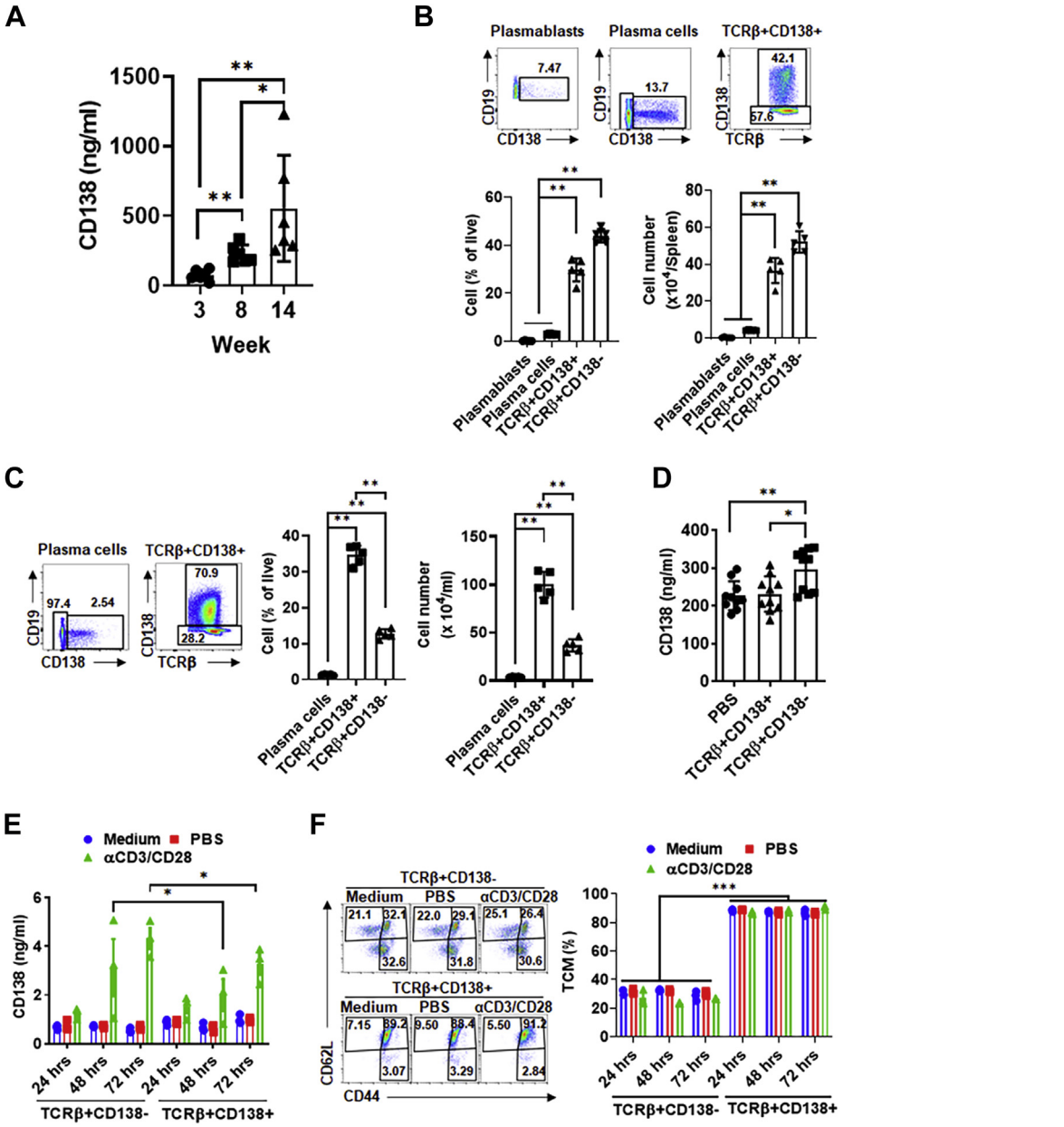

Figure 1. Activated TCRβ+CD138− cells secrete more CD138 than TCRβ+CD138+ cells do. *A*, serum CD138 levels in MRL/Lpr mice from different ages were measured by ELISA. Mean ± SD of six mice from two independent experiments are plotted. *B* and *C*, splenic (*B*) or blood (*C*) plasmablasts (CD19+CD138+), plasma cells (CD19−CD138+), and TCRβ+CD138+ cells were characterized and enumerated from 14-week-old MRL/Lpr mice. Mean ± SD of five mice from two independent experiments are plotted. *D*, purified TCRβ+CD138− or TCRβ+CD138+ cells from 12- to 14-week-old MRL/Lpr mice were adoptively transferred into 8-week-old MRL/Lpr mice, and the serum CD138 levels were determined by ELISA 3 days after the transfer. Mean ± SD of ten mice from two independent experiments are plotted. *E*, TCRβ+CD138− and TCRβ+CD138+ cells were purified from 12- to 14-week-old MRL/Lpr mice and activated for indicated durations. Culture supernatant CD138 levels were measured by ELISA. Mean ± SD of three mice from three independent experiments are plotted. *F*, TCRβ+CD138− and TCRβ+CD138+ cells were purified from 12- to 14-week-old MRL/Lpr mice activated for indicated durations and TCM (CD44+CD62L+), TN (CD44−CD62L+), and TEM (CD44+CD62L−) subsets were measured in FACS. Representative FACS images of 72-h treated cells and the frequency of TCM cells at three time points are shown. Mean ± SD of three mice from three independent experiments are plotted. *$p < 0.05$, **$p < 0.01$, and ***$p < 0.001$. FACS, fluorescence-activated cell sorting; TCM, central memory T; TCRβ, T-cell receptor β; TEM, effector memory T; TN, naive T.

short-term (5-min) treatment with trypsin or TrypLe, cell surface CD138 expression sharply decreased on TCRβ+CD138+ cells (Fig. 2*C* and Fig. S2, *D* and *E*). Supporting the observed trypsin activity, analysis of mouse CD138 amino acid sequence indicated that there are 13 arginine and lysine amino acids in the extracellular domain of CD138, all of which are potential trypsin targets (Fig. S2*F*). Moreover, two of trypsin targets are just located at the C-terminal region of CD138 ectodomain (Fig. S2*F*). To verify the trypsin cleavage and release of CD138 from TCRβ+CD138+ cells, we measured the CD138 content in the supernatants from short-term trypsin-treated cells by ELISA. Compared with the supernatants from untreated cells, significantly higher levels of soluble CD138 were detected in the supernatants of trypsin-treated

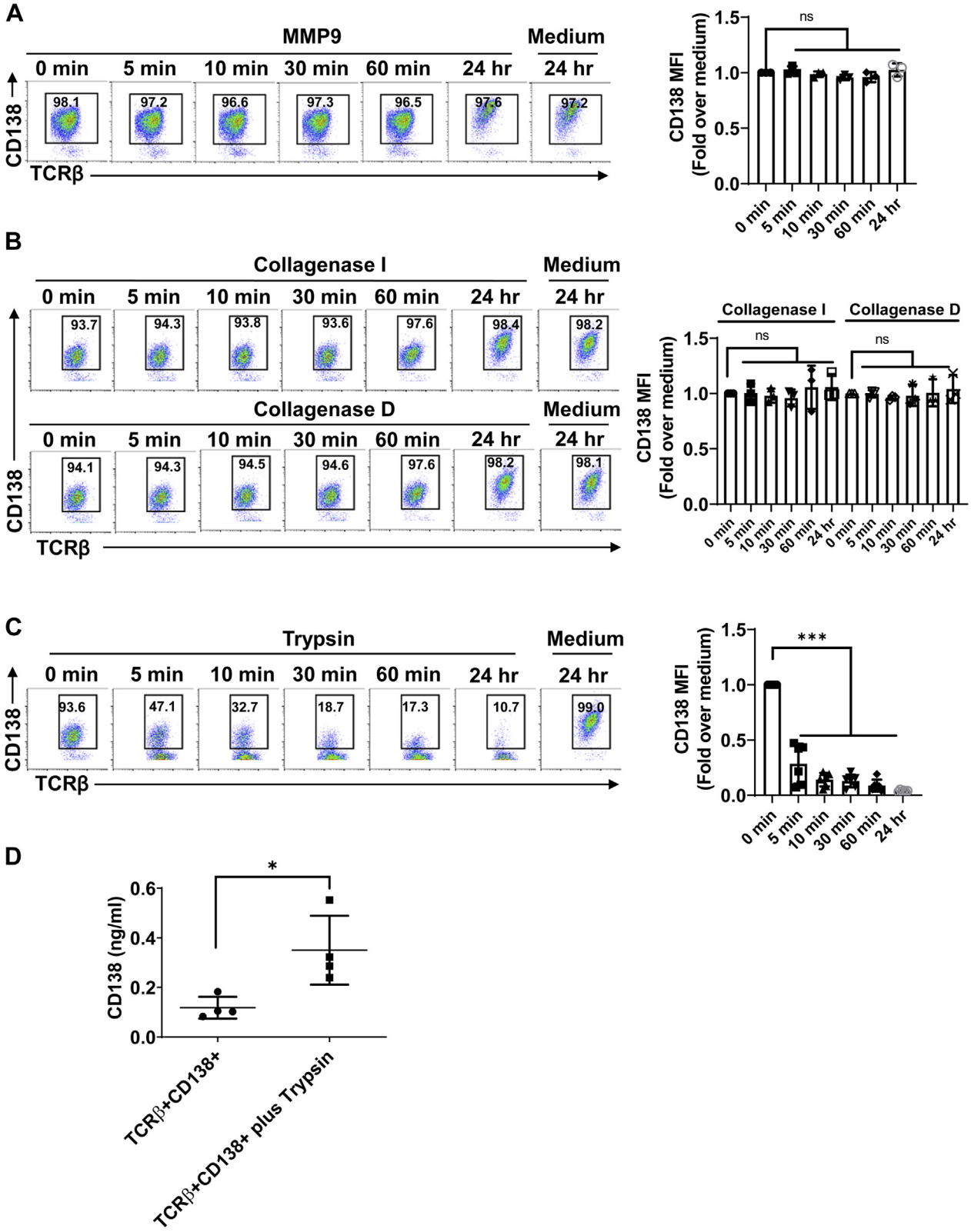

Figure 2. CD138, on TCRβ+CD138+ cells, is sensitive to cleavage by trypsin. Purified TCRβ+CD138+ cells from 12-week-old MRL/Lpr mice were treated with active MMP9 (*A*), collagenase I and D (*B*), or trypsin (*C*) for indicated durations, and CD138 mean fluorescence intensity (MFI) levels on treated cells were measured by FACS. Mean ± SD of 3 to 6 independent experiments are plotted. *D*, purified TCRβ+CD138+ cells from 12-week-old MRL/Lpr mice were treated with trypsin for 5 min, and culture supernatant CD138 levels were measured by ELISA. Mean ± SD of four independent experiments are plotted. *$p < 0.05$ and ***$p < 0.001$. FACS, fluorescence-activated cell sorting; MMP9, matrix metalloproteinase 9; ns, not significant; TCRβ, T-cell receptor β.

cells (Fig. 2*D*). Thus, CD138 on lupus T cells is highly sensitive to trypsin cleavage but resistant to MMP9 and collagenases.

Trypsin expressed by TCRβ+CD138− cells constitutively sheds CD138 from these cells

Although pancreas is the primary source of serine protease trypsin, active trypsin is also present in mouse and human spleen cells (31). To assess whether lupus T cells also produce trypsin, we measured trypsin mRNA expression in splenic T cells and found higher trypsin gene expression in TCRβ+CD138− cells than TCRβ+CD138+ cells purified from 10- to 12-week-old MRL/Lpr mice (Fig. 3*A*). We confirmed the higher trypsin protein production in TCRβ+CD138− cells than TCRβ+CD138+ cells isolated from both 8- and 14-week-old MRL/Lpr mice by Western blot analysis (Fig. 3*B*). Also, the level of trypsin increased with age in both T-cell subsets, paralleling the disease progression with age typically seen in MRL/Lpr mice. Moreover, αCD3/CD28 antibody (Fig. 3*C* and Fig. S3*A*) or phenylmercuric acetate (PMA) and ionomycin (Ion) (Fig. S3*B*) stimulation increased the levels of trypsin production in both TCRβ+CD138+ and TCRβ+CD138− cells, although the

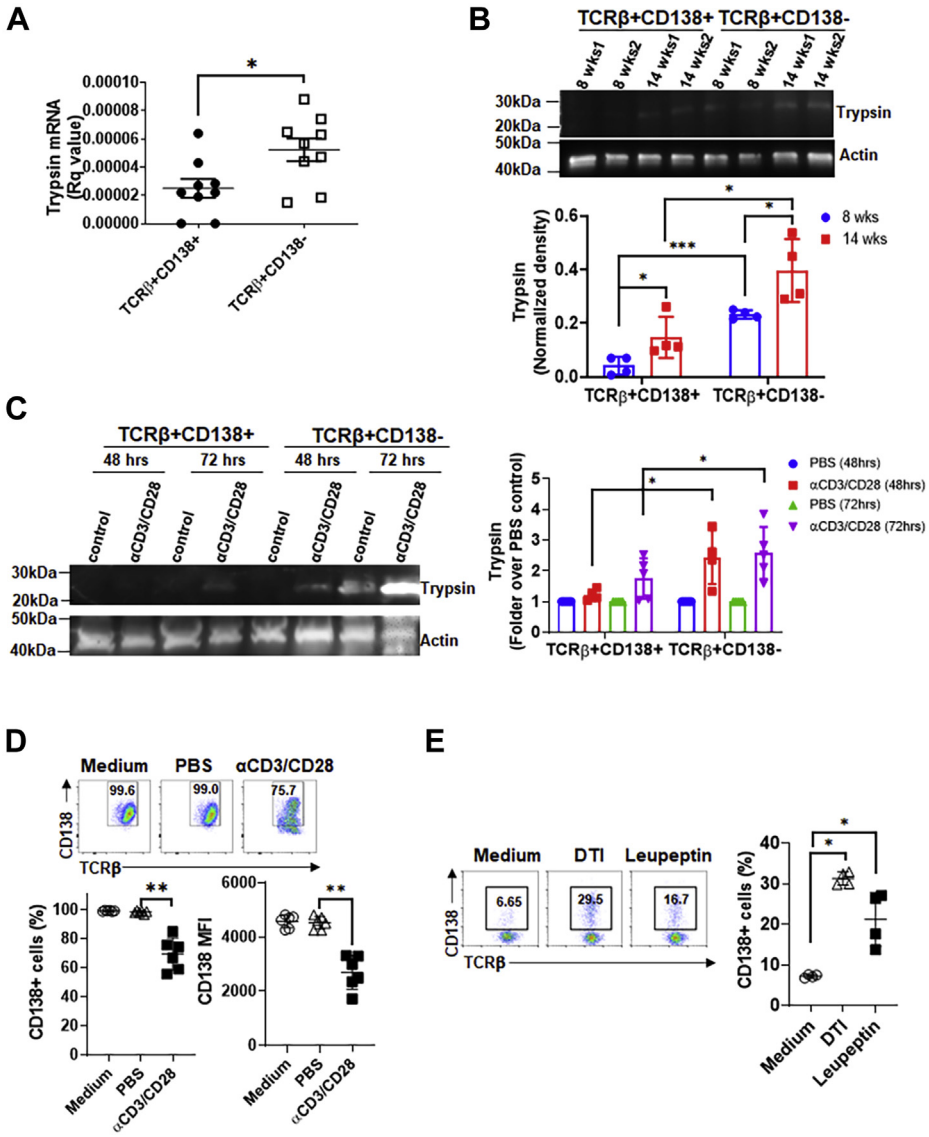

Figure 3. Lupus mouse splenic T cells produce biologically active trypsin. *A*, trypsin mRNA levels in splenic TCRβ+CD138+ and TCRβ+CD138− cells purified from 10- to 12-week-old MRL/Lpr mice were quantified by quantitative PCR. Mean ± SD of nine samples per group are plotted. *B*, trypsin protein was detected in splenic TCRβ+CD138+ and TCRβ+CD138− cells purified from 8- to 14-week-old MRL/Lpr mice by Western blot analysis. Samples from two mice on each time point are shown. The band intensities were quantified with ImageJ program. Mean ± SD of four different samples are plotted. *C*, purified TCRβ+CD138+ and TCRβ+CD138− cells from 10- to 12-week-old MRL/Lpr mice were treated with αCD3/CD28 antibodies for 48 or 72 h, after which trypsin expression was detected by Western blot analysis. The band intensities were quantified with ImageJ program. Mean ± SD of 4 to 5 different samples are plotted. *D*, purified TCRβ+CD138+ cells from 10- to 12-week-old MRL/Lpr mice were treated with αCD3/CD28 antibodies for 48 h, and membrane CD138 expression was measured by FACS. Mean ± SD of six different samples are plotted. *E*, purified TCRβ+CD138− cells from 10- to 12-week-old MRL/Lpr mice were cultured in serum-free medium (without stimulation) and treated with trypsin inhibitors, DTI and leupeptin, for 24 h, after which the frequencies of CD138-expressing cells were measured by FACS. Mean ± SD of four different samples are plotted. *$p < 0.05$, **$p < 0.01$, and ***$p < 0.01$. DTI, defined trypsin inhibitor; FACS, fluorescence-activated cell sorting; TCRβ, T-cell receptor β.

increases in TCRβ+CD138− cells were higher. Coinciding with the increase in trypsin production in stimulated cells, we found a significant decrease in the expression of membrane CD138 on αCD3/CD28 antibody-treated TCRβ+CD138+ cells (Fig. 3*D*). A similar decrease in CD138 expression was also observed in PMA/Ion-treated TCRβ+CD138+ cells (Fig. S3*C*). The simultaneous increase in the trypsin production and the decrease in CD138 expression on trypsin-treated TCRβ+CD138+ cells suggest the cleavage of CD138 by the trypsin produced from TCRβ+CD138− cells. To test this hypothesis, we cultured TCRβ+CD138− cells in serum-free medium and blocked the intrinsic trypsin activity by adding the trypsin inhibitors, defined trypsin inhibitor or leupeptin. Although the inhibitors led to some cell death (Fig. S3*D*), TCRβ+CD138− cells expressed significantly higher CD138 after treatment with both the inhibitors (Fig. 3*E*). Moreover, this effect was trypsin inhibitor specific as no remarkable change in CD138 expression was observed in TCRβ+CD138− cells treated with inhibitors specific for MMP9 and focal adhesion kinase (Fig. S3*E*). These results indicate that higher expression of intrinsically active trypsin in TCRβ+CD138− cells could be responsible for the shedding of CD138 from T cells in lupus mouse and contribute to the accumulation of CD138 in the MRL/Lpr mouse blood.

Soluble CD138 containing serum enhances B-cell differentiation and ERK activation

We next sought to investigate the function of soluble CD138 in lupus mouse serum. We first removed CD138 from serum by using anti-CD138 antibody-conjugated beads (Fig. 4*A*) and tested CD138-depleted serum-mediated B-cell differentiation. When B cells were stimulated with APRIL and lipopolysaccharide (LPS) in CD138-depleted serum, $B220^{int}$CD138+ plasma cell formation was significantly reduced as compared with cells cultured in serum that was treated with IgG beads only (Fig. 4*B*). The activity of CD138 on B-cell differentiation was further confirmed by CD138 reconstitution experiment. Supplementation of CD138-depleted lupus mouse serum with 300 ng/ml of mouse CD138 significantly increased $B220^{int}$CD138+ plasma cell development in APRIL- and LPS-stimulated B cells compared with cells stimulated with CD138-depleted serum (Fig. 4*C*). Importantly, these $B220^{int}$CD138+ cells also exhibited elevated CXCR4 expression, an important molecule for plasma cell trafficking and maintenance (32, 33). The expression of CXCR4 on plasma cells suggests that the measurement of elevated CD138 expression on B220 cells is not a result of reconstituted CD138 binding to B220 cells but is due to the differentiation of B cells into plasma cells (Fig. S4). The ERK signaling mediates key molecular switches controlling B-cell differentiation (34). Since we found that lupus mouse CD138 levels increase with age and serum CD138 promotes plasma cell development, we wanted to examine whether sera from older lupus mice activate ERK pathway more than the younger mice do. Supporting this hypothesis, we found an age-dependent increase in ERK phosphorylation after treatment of B cells with sera from 3-, 8-, and 14-week-old lupus mice (Fig. 4*D*). We verified the contribution of CD138 in lupus mouse serum induced ERK phosphorylation by comparing the ERK activation in B cells incubated with serum before and after CD138 depletion. Compared with unmanipulated sera, sera depleted of CD138 induced significantly less ERK phosphorylation (Fig. 4*E*). Collectively, ERK phosphorylation experiments underscore the contribution of CD138 in lupus mouse serum-mediated differentiation of B cells.

Soluble CD138 binds to APRIL and enhances APRIL-induced B-cell differentiation and ERK activation

In CD138-transfected Jurkat T cells and CD138-positive myeloma cells, APRIL, but not BAFF, has been shown to specifically bind heparin chain of membrane-bound CD138, but, to our knowledge, the binding of APRIL or BAFF to soluble CD138 has not been reported (35, 36). Using CD138 antibody-coated beads, we found that CD138 antibodies can pull down APRIL when CD138 and APRIL are coincubated (Fig. S5*A*). Like serum CD138, both serum APRIL and BAFF levels increase in lupus mice as the disease progresses with age (Fig. S5*B*). Paralleling the increase in serum APRIL, we found that anti-CD138 antibody-coupled beads coimmunoprecipitated higher amounts of APRIL from the sera of older lupus mice than younger mice (Fig. 5*A*). When tested for APRIL levels, sera treated with anti-CD138 antibody-coupled beads had drastically reduced levels of APRIL after the depletion of CD138 (Fig. 5*B*). Conversely and underscoring the specificity of CD138 for APRIL, serum BAFF levels remained unchanged after the pull down with anti-CD138 antibody-coupled beads (Fig. 5*B*). Thus, like its membrane-bound counterpart, soluble CD138 also specifically binds to APRIL.

Both APRIL and BAFF induce ERK activation (Fig. 5*C*) (37), a critical signal for B-cell survival and differentiation (38, 39). We next tested whether soluble CD138 modulates BAFF- and APRIL-induced ERK phosphorylation in B cells. Although soluble CD138 itself induced minimal ERK phosphorylation, costimulation of B cells with CD138 and APRIL profoundly enhanced APRIL-mediated ERK activation (Fig. 5*C*). Moreover, reconstitution of CD138-depleted lupus mouse serum with CD138 led to enhanced ERK phosphorylation with APRIL (Fig. S5*C*). This potentiation effect is unique to APRIL, as combination of BAFF and soluble CD138 did not exhibit any synergy on ERK activation (Fig. 5*C*). As expected, combination of APRIL, but not BAFF, with CD138 resulted in improved lupus B-cell survival (Fig. 5*D*). Both BAFF and APRIL have been shown to enhance B-cell differentiation and stimulation of immunoglobulin G (IgG), IgM, and IgA secretion (37). Once again, while combining BAFF with CD138 did not change the percentage of plasma cells induced by BAFF, lupus B cells stimulated with APRIL and CD138 differentiated into plasma cells more than those stimulated with APRIL alone (Fig. 5*E*). Combination of APRIL with CD138 also augmented anti-dsDNA antibody production from lupus B cells (Fig. 5*F* and Fig. S5*D*). It should be noted that incubation of B cells with CD138 and APRIL did not significantly increase total IgG, total IgA, and anti-dsDNA IgA antibody production as compared with cells stimulated with APRIL alone, but it did elicit

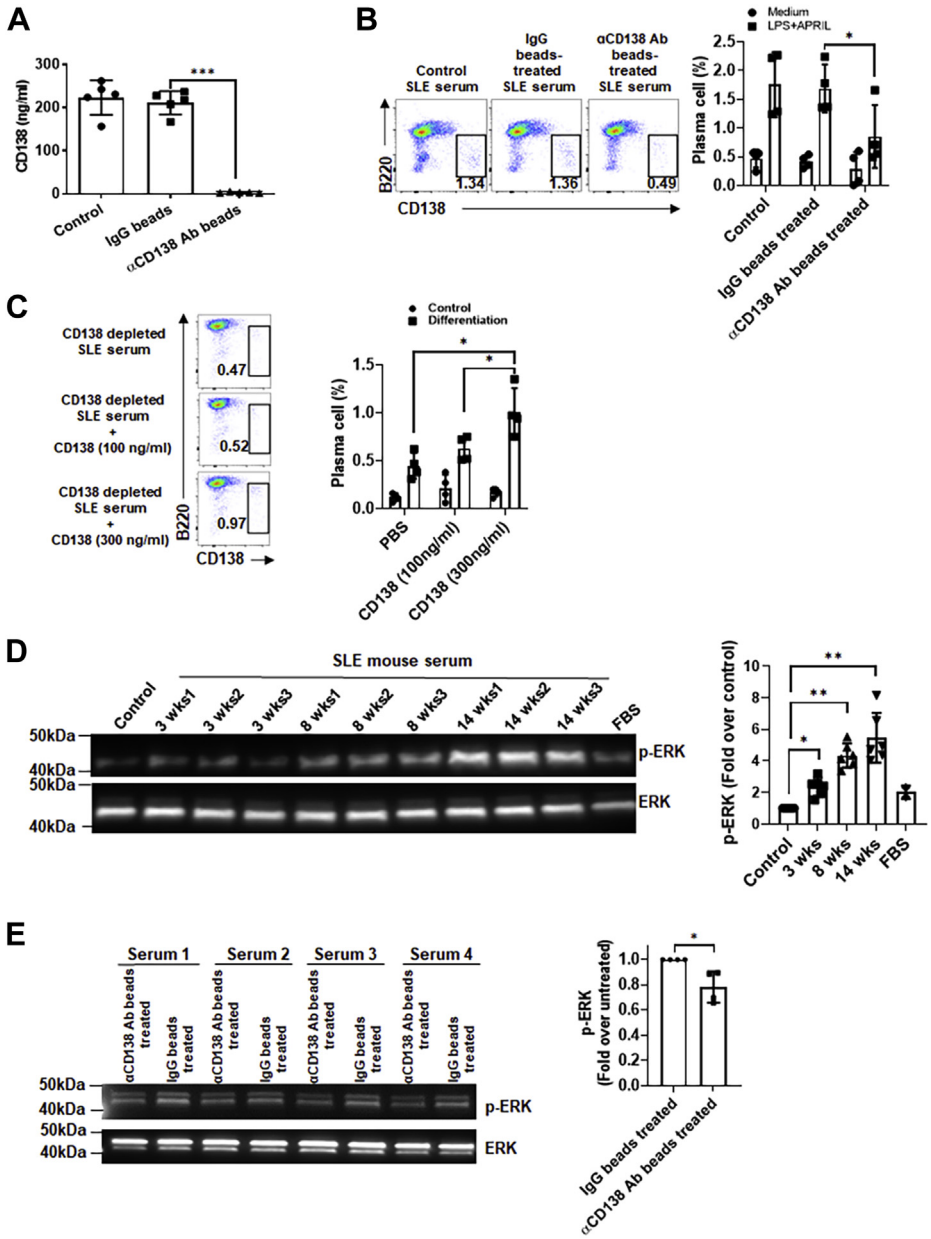

Figure 4. Depletion of serum CD138 in lupus mouse blunts serum-induced B-cell differentiation and ERK activation. *A*, sera from 14-week-old MRL/Lpr mice were left untreated (control) and treated with protein A/G beads coupled to IgG or CD138 antibody. The remaining soluble CD138 in the serum was quantified in ELISA. Mean ± SD of five independent experiments are plotted. *B*, B cells from 10- to 12-week-old lupus mice were cultured with APRIL plus LPS for 5 days in RPMI medium containing either 10% untreated (control) lupus mouse serum and lupus mouse serum pretreated with IgG beads or anti-CD138 antibody beads. After 5 days, frequencies of plasma cells ($B220^{int}$ CD138+) were quantified by FACS analysis. Mean ± SD of four independent experiments are plotted. *C*, B cells from 10- to 12-week-old lupus mice were cultured in CD138-depleted lupus mouse serum with or without addition of mouse CD138 at indicated concentrations. After 5 days of incubation, plasma cell development was assessed by FACS analysis. Mean ± SD of four independent experiments are plotted. *D*, lupus mouse B cells cultured in RPMI medium were left untreated (control) and treated with 10% FBS or with 10% serum samples from 3-, 8-, and 14-week-old lupus mice (three separate mice for each age group) for 24 h. ERK phosphorylation was assessed by Western blot analysis, and the band intensity was quantified with ImageJ program. Mean ± SD of 1 to 3 independent samples are plotted. *E*, lupus mouse B cells were incubated for 16 h with 10% lupus mice (14 weeks old) sera that were untreated or treated with anti-CD138 antibody beads prior to incubation. ERK phosphorylation was assessed by Western blot analysis, and the band intensity was quantified with ImageJ program. Mean ± SD of four different samples are plotted. *$p < 0.05$ and **$p < 0.01$. APRIL, a proliferation-inducing ligand; ERK, extracellular signal–regulated kinase; FACS, fluorescence-activated cell sorting; FBS, fetal bovine serum; LPS, lipopolysaccharide.

significantly higher levels of total IgM, anti-dsDNA IgM, and anti-dsDNA IgG antibodies (Fig. 5*F* and Fig. S5*D*). These results indicate that binding of soluble CD138 to APRIL amplifies APRIL-induced signaling, which ultimately leads to increased differentiation of autoreactive B cell into antibody-secreting plasma cells in lupus mouse.

Both BAFF and APRIL share receptors TACI and BCMA on B cells (40). In primary multiple myeloma cells, membrane CD138 has been shown to function as a coreceptor for APRIL and TACI and promote cell survival and proliferation through the APRIL–TACI pathway (35). Consistent with these findings, although not completely, TACI deficiency significantly impaired

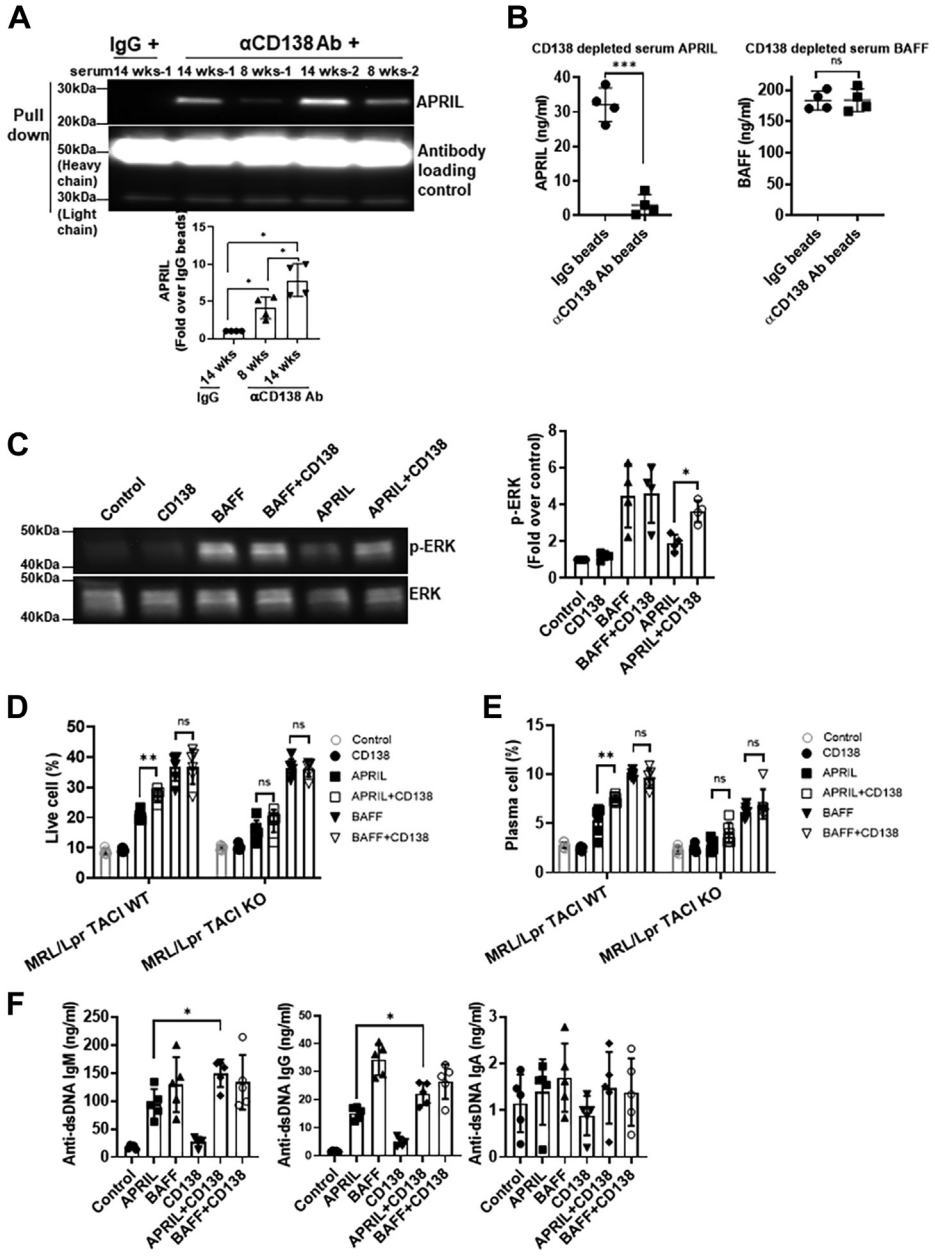

Figure 5. CD138 potentiates APRIL-induced ERK activation and B-cell differentiation. *A*, sera from 8- and 14-week-old lupus mice were subjected to immunoprecipitation using CD138-specific antibody and protein A/G-Sepharose beads. Sera from 14-week-old mice with rabbit IgG was also precipitated as control. Precipitates were resolved by SDS-PAGE and analyzed by immunoblotting using APRIL-specific antibodies as indicated. Mean ± SD of four independent experiments are plotted. *B*, APRIL and BAFF levels were quantified by ELISA after treatment of 14-week-old lupus mice sera in section *A*. Mean ± SD of 8 to 11 samples are plotted. *C*, B cells from 10- to 12-week-old lupus mice were cultured in 10% FBS RPMI medium for 1 h first and then treated with APRIL, BAFF, CD138 alone, or with BAFF plus CD138 and APRIL plus CD138. After 24 h stimulation, ERK phosphorylation was evaluated by Western blot analysis, and the band intensities were quantified with ImageJ program. Mean ± SD of four independent experiments are plotted. *D* and *E*, splenic B cells isolated from 10- to 12-week-old MRL/Lpr TACI WT or MRL/Lpr TACI KO mice were cultured in 10% FBS RPMI medium for 1 h and then treated with APRIL, BAFF, CD138 alone, or in combination with APRIL and CD138 or BAFF and CD138. After 5 days, cell viability (*D*) and plasma cell formation (*E*) were assessed by FACS. Mean ± SD of six independent experiments are plotted. *F*, lupus mouse B cells were treated as in *D* and *E*. After 5 days, anti-dsDNA–specific antibody levels in the culture supernatants were quantified by ELISA. Mean ± SD of five independent experiments are plotted. $^{*}p < 0.05$, $^{**}p < 0.01$, and $^{***}p < 0.001$. APRIL, a proliferation-inducing ligand; BAFF, B-cell–activating factor; ERK, extracellular signal–regulated kinase; FACS, fluorescence-activated cell sorting; FBS, fetal bovine serum; ns, not significant; TACI, transmembrane activator, calcium modulator, cyclophilin ligand interactor.

the potentiation effect of CD138 on APRIL-stimulated B-cell survival (Fig. 5*D* and Fig. S5*E*) and differentiation into plasma cells (Fig. 5*E* and Fig. S5*F*). We suspect that soluble CD138 enhances APRIL activity by oligomerizing multiple APRIL molecules. Since APRIL oligomers have higher affinity to its receptors BCMA and TACI (41), soluble CD138-bound APRIL likely induces higher ERK activation, B-cell survival, and differentiation through these receptors than monomeric APRIL does.

Discussion

In this study, we reported the augmentation of APRIL-mediated B-cell survival, differentiation, and ERK

phosphorylation by soluble CD138. Our study also identified the involvement of TACI in the enhanced activity of soluble CD138-bound APRIL, as lupus B cells lacking TACI responded weaker to APRIL even when coincubated with soluble CD138. Although TCRβ+CD138+ cells increasingly populate lupus mouse as the disease progresses, our data strongly point to CD138-negative T cells as the primary source of soluble serum CD138 in lupus mouse because *in vitro*–activated TCRβ+CD138– cells released more CD138 into the medium than TCRβ+CD138+ cells did. In support of these *in vitro* experiments, we have shown that lupus mice injected with TCRβ+CD138– cells accumulate more serum CD138 than those injected with TCRβ+CD138+ cells. Elevated production of soluble CD138 from TCRβ+CD138– cells was due to their high intrinsic trypsin production as membrane CD138 on lupus T cells was very sensitive to trypsin cleavage, and blocking of trypsin led to CD138 retention on TCRβ+CD138– cell membrane (Fig. 6).

Membrane CD138 is expressed at high levels in epithelial cells, plasmablasts, plasma cells, and various cancer cells such as those from lung squamous cancer, adenocarcinoma, head and neck squamous cancer, and mesothelioma (21, 22, 42, 43). High level of circulating soluble CD138 has been reported in patients with multiple myeloma, lung cancer, and SLE (5, 6, 21, 44). The presence of soluble CD138 in the serum of patients with multiple myeloma and SLE was believed be the result of constitutive shedding of CD138 from plasma cells (5, 22). Previously, we reported the expression of CD138 on a big portion of central memory TCRβ+ cells in MRL/Lpr mice (23). Accumulation of these CD138-positive T cells together with the exposure of autoantigens results in the activation of host immune system and production of autoreactive antibodies in lupus mice.

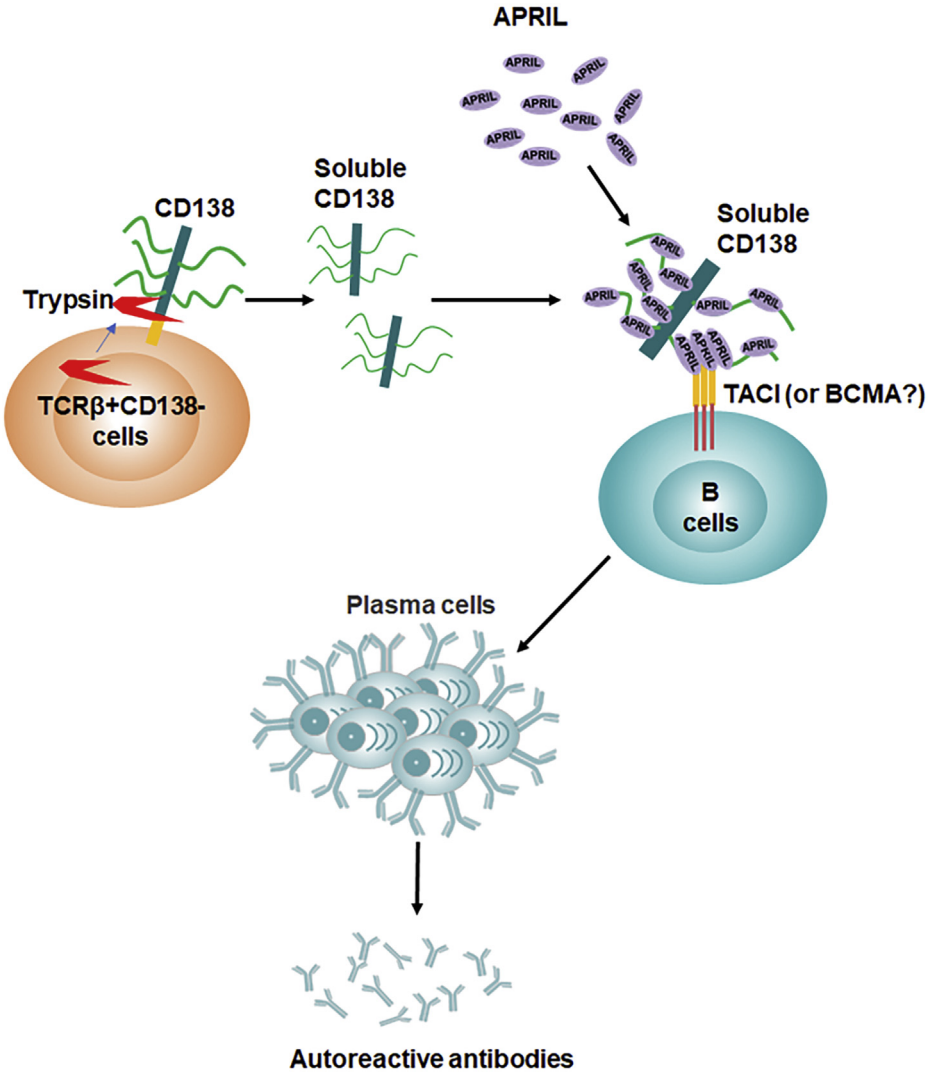

Figure 6. The origin and function of soluble CD138 in lupus disease. Some of the TCRβ+CD138– cells derive from a subset of activated trypsin-expressing TCRβ+CD138+ cells as a result of the cleavage of membrane CD138 by trypsin. The released soluble CD138 binds and aggregates APRIL to form APRIL oligomers, which is known to increase its binding affinity to the receptor TACI or BCMA. We have shown that binding of APRIL oligomers to TACI enhances lupus B-cell survival and differentiation into antibody-secreting plasma cells. Thus, soluble CD138 likely promotes lupus progression by augmenting autoreactive antibody production. APRIL, a proliferation-inducing ligand; BCMA, B-cell maturation antigen; TACI, transmembrane activator, calcium modulator, cyclophilin ligand interactor; TCRβ, T-cell receptor β.

Despite expressing elevated levels of CD138, our study showed that TCRβ+CD138+ cells release less CD138 into the blood as compared with TCRβ+CD138− cells. In malignancies such as breast cancer and myeloma, CD138 ectodomain is believed to be shed by MMPs or collagenases produced by cancer cells (11, 13, 28, 29). Here, we showed that these proteinases are unlikely to contribute to the cleavage of membrane CD138 from lupus T cells as CD138 on these cells was resistant to digestion by these enzymes. Instead, we found that T-cell CD138 was very sensitive to trypsin treatment. Moreover, resting and activated TCRβ+CD138− cells expressed relatively high levels of trypsin, and the trypsin released from these cells effectively shed CD138 from lupus T cells in an autocrine fashion. Thus, the cleavage of CD138 from these T-cell subsets by intrinsically active trypsin is likely to be responsible for the accumulation of CD138 in the lupus mouse blood.

By binding to extracellular matrix components, integrins, growth factors, cytokines, and chemokines, membrane-bound CD138 could regulate multiple biological processes, such as wound healing, cell adhesion, endocytosis, vesicular trafficking, angiogenesis, and apoptosis (7). The intracellular C1 and C2 regions of membrane-bound CD138 are critical for these functions as their interaction with cytoskeleton, Src kinase, or other adaptor proteins can initiate multiple downstream signaling cascades (7, 42). Even though the soluble CD138, ectodomain of whole protein, lack these two vital intracellular domains, several lines of evidence indicate that soluble CD138 could also be biologically active as both competitive inhibitors and agonists. For example, soluble CD138 is shown to inhibit the mitogenicity of fibroblast growth factor 2, decrease the growth of carcinoma cells, and induce apoptosis in myeloma cells *in vitro* (16, 17, 45, 46). Conversely, CD138 ectodomain promotes *in vivo* tumor cell invasion as well as myeloma growth by facilitating the binding of very late antigen-4 to vascular endothelial growth factor receptor 2 (20, 47). Similar to the function reported for membrane CD138, which provides survival advantage to myeloma or plasma cells by potentiating APRIL signaling (43), we also found an enhancement of APRIL function in inducing ERK activation and B-cell differentiation when soluble CD138 is present. Importantly, soluble CD138 did not provide a detectable enhancement of BAFF activity as no increase in cell survival, differentiation, and antibody secretion was observed in B cells treated with BAFF in the presence of CD138. Moreover, as in CD138 expressed on membrane of human embryonic kidney 293 cells, Jurkat cells, and primary multiple myeloma cells, which exhibit strong binding to APRIL but not to BAFF (35, 36), we also observed coprecipitation of APRIL with soluble CD138. Although we do not know the exact number of APRIL molecules binding to CD138, previous reports indicated that thousands of epidermal growth factors and APRIL molecules can bind to membrane syndecan-1 through its heparan sulfate chain (35, 48). Thus, the enhancement of APRIL activity by soluble CD138 is likely a result of the oligomerization of CD138-bound APRIL molecules (Fig. 6).

Previous studies reported the binding of membrane CD138, syndecan-2, and syndecan-4 to TACI (35, 49). It is possible that soluble CD138 can augment APRIL activity by simultaneously binding to both APRIL and its receptor TACI. Suggesting a partial involvement by TACI, the enhancement mediated by CD138 on APRIL induced signaling, cell survival, and autoreactive antibody production was decreased but not totally abolished in TACI-deficient MRL/Lpr mice B cells. Since APRIL engages BCMA in addition to TACI, and BCMA is involved in plasma cell generation and maintenance (50, 51), both TACI and BCMA likely mediate APRIL oligomer activity.

Previously, we reported a pathogenic role for TCRβ+CD138+ cells with central memory phenotype in MRL/Lpr mice (23). We showed that TCRβ+CD138+ cells can activate autoreactive B cells upon antigen encounter (23). Underscoring the T-cell–dependent activation of B cells during antigen presentation, the stimulation of autoreactive B cells required CD4 expressed on TCRβ+CD138+ cells. Both SLE patients (5, 6) and lupus mouse (current study) present with an increase in blood CD138 as the disease progresses. Building on our previous study, we now show that CD138 released from TCRβ+CD138− cells not only contributes to the increase in circulating CD138 pool but also participates in the activation of B cells by aggregating the T-cell–independent B-cell activator, APRIL (3), and potentiating its activity on B cells (Fig. 6). Thus, both CD138+ and CD138− T cells contribute to lupus pathology through distinct pathways. These findings highlight a previously unappreciated participation of CD138 in lupus pathogenesis, which may be exploited to evaluate disease progression and/or may unveil novel therapeutic targets.

Experimental procedures

Mice

MRL/MpJ-FASLPR/J (referred to as MRL/Lpr throughout the article) were purchased from The Jackson Laboratory. TACI-deficient MRL/Lpr mice (MRL/Lpr TACI KO) and the WT counterpart (MRL/Lpr TACI WT) were described previously (26). All mice were bred and housed under specific pathogen-free conditions in the animal facility of US Food and Drug Administration/Center for Biologics Evaluation and Research Veterinary Services. The use of animals was approved by and carried out within accordance of the US Food and Drug Administration/Center for Biologics Evaluation and Research Institutional Animal Care and Use Committee (permit numbers 2002-31 and 2017-47). All methods were performed in accordance with the relevant guidelines and regulations.

Flow cytometry

Single cell suspensions of spleens were prepared by mechanical dissociation of tissue through a 40-μm cell strainer. Red blood cells were then lyzed using ammonium–chloride–potassium lyses buffer (Lonza). Mouse blood leukocytes were collected by lysing red blood cells with ammonium–chloride–potassium buffer and centrifugation at 300*g* for 5 min. Cells were stained with fluorescent-labeled antimouse antibodies after blocking CD16/CD32 with Fc Block (BD Biosciences). Flow cytometry analysis was performed using

following antibodies: Pacific blue anti-CD19, BV421 anti-CD19, APC anti-TCRβ, APC CXCR4, Percp Cy5.5 B220 (all from BioLegend), and PE–anti-CD138 (from BD biosciences). 4′,6-diamidino-2-phenylindole (DAPI) and LIVE/DEAD Fixable Near-IR Dead Cell Stain Kit were purchased from Thermo Fisher Scientific. APRIL-Alexa488 and bovine serum albumin-Alexa488 were prepared by conjugation of APRIL and bovine serum albumin to Alexa Fluor 488 NHS ester (Thermo Fisher). Stained cells or beads were analyzed using a flow cytometer (LSR II; BD), and data were analyzed using FLOWJO, version 10.1, for PC (Tree Star).

Measurement of CD138, APRIL, and BAFF production

CD138 levels in MRL/Lpr mice serum or culture supernatants were measured using mouse SDC1 ELISA Kit from Aviva Systems Biology according to the manufacturer's instructions. Serum APRIL and BAFF levels in MRL/Lpr mice blood were measured using mouse APRIL ELISA kit (Mybiosource) and mouse BAFF/BLyS/TNF13B DuoSet ELISA kit (R&D Systems), respectively.

MMP9 activity measurement

Recombinant mouse MMP9 protein was purchased from Abcam. To obtain maximum latent MMP9, MMP9 was treated with 2.5 mM 4-aminophenylmercuric acetate (Sigma–Aldrich) in a buffer containing 50 mM Tris–HCl, pH 7.5, 1 mM $CaCl_2$, and 0.05% Triton X-100 at 37 °C for 1 h prior to use. The activity of MMP9 was verified with MMP9 colorimetric drug discovery kit (Enzo) according to the manufacturer's instructions.

T-cell isolation and stimulation

MRL/Lpr mice splenic T cells were purified with Dynabeads FlowComp Mouse Pan T (CD90.2) Kit and dissociated from beads according to manufacturer's instructions (Thermo Fisher). After staining purified T cells with PE anti-CD138 antibody, TCRβ+CD138– and TCRβ+CD138+ cells were further separated with anti-PE magnetic microbeads (Miltenyi Biotec). Depending on the experimental objective, purified TCRβ+CD138+ and TCRβ+CD138– cells were stimulated with 1 μg/ml anti-CD3 and anti-CD28 antibodies (BD Pharmingen), 10 ng/ml PMA and 100 ng/ml Ion, 100 mg/ml collagenase I, 100 mg/ml collagenase D, 2.5 mg/ml trypsin, 10 μM leupeptin, 500 μM aminophenyl mercuric acetate (all from Sigma–Aldrich), 10 μM focal adhesion kinase inhibitor 14 (Cayman chemicals), 10 μg/ml MMP9, TrypLE, or defined trypsin inhibitor (all from Thermo Fisher) for indicated duration, and the expression levels of cell surface CD138 were quantified by fluorescence-activated cell sorting (FACS). Trypsin gene expression levels were quantified by quantitative PCR, and trypsin protein was analyzed by Western blot using rabbit polyclonal trypsin antibody (Thermo Fisher).

T-cell adoptive transfer experiments

Purified TCRβ+CD138– and TCRβ+CD138+ cells were washed three times with PBS before resuspending them in PBS. MRL/Lpr mice were injected i.v. with 1×10^7 cells in 100 μl of PBS.

B-cell isolation and stimulation

Splenic B cells were isolated from 10- to 12-week-old MRL/Lpr mice using B Cell Isolation Kit (Miltenyi Biotec). Isolated cells were washed three times with PBS, after which their purity was assessed by flow cytometry (purity was greater than 97%). For B-cell stimulation and survival, 1×10^6 B cells were cultured in RPMI media containing 2 to 10% fetal bovine serum or 10% of anti-CD138 beads pretreated or IgG-coated beads pretreated MRL/Lpr mice serum. Next, cells were stimulated with 500 ng/ml of recombinant APRIL (Peprotech) or recombinant BAFF (R&D Systems) with or without recombinant mouse CD138 (R&D Systems) for 24 or 120 h. Phosphorylation of ERK was assessed in Western blot analysis, and the survival of cells was analyzed by FACS after DAPI staining. For B-cell differentiation analysis, B cells were first cultured in RPMI media containing 10% anti-CD138 beads pretreated MRL/Lpr mice serum with, and then were incubated with 250 ng/ml of APRIL and 10 ng/ml of LPS for 5 days. Stimulated cells were harvested, and percentages of plasma cells were assayed on DAPI-negative cells with FACS after staining with B220, CD138, and CXCR4 antibodies. Culture supernatants were also collected, and total or anti-dsDNA–specific IgM, IgG, and IgA antibody concentrations were determined in ELISA as described previously (26).

Immunoprecipitation and immunoblotting

For immunoprecipitation, 200 μl of serum samples were first prediluted with 1 ml cold RIPA buffer containing halt protease and phosphatase inhibitor cocktail (Thermo Scientific), and then rotated with IgG or CD138 antibody-precoated protein A/G beads at 4 °C for 1.5 h. Next, beads were washed three times with cold RIPA buffer and once with cold PBS. Samples were resuspended in 30 μl of NuPAGE LDS-Sample buffer (Thermo Fisher) and separated by 4 to 20% SDS-PAGE (Bio-Rad). For immunoblotting, purified splenic B cells, TCRβ+CD138– or TCRβ+CD138+ cells were initially washed twice with cold PBS and then lyzed on ice with LDS-sample buffer for 15 min. After boiling, solubilized materials were resolved on 4 to 20% SDS-PAGE and transferred to polyvinylidene fluoride membranes using a semidry transfer system (Thermo Fisher). Membranes were blocked with 5% nonfat dried milk in Tris-buffered saline plus Tween-20 and incubated with the indicated primary antibodies (1:1000) overnight at 4 °C. Next day, the membranes were washed four times for 10 min in Tris-buffered saline plus Tween-20 and then incubated with 1:5000 diluted goat anti-rabbit IgG conjugated to horseradish peroxidase for 1 h at room temperature. Protein bands were imaged with FluorChem systems (Alpha Innotech).

Quantitative real-time PCR

Total RNA was extracted from the FACS cells using RNeasy Mini kit (Qiagen). Two hundred nanograms of total RNA were

reverse transcribed into complementary DNA using random hexamers with the Taqman Reverse Transcription Kit (Thermo Fisher). The expression of targeted genes and GAPDH was determined using Taqman gene expression assays (Thermo Fisher) and CFX96 Touch Real-Time System (Bio-Rad). Relative expression values were determined by the 2-ΔCt method where samples were normalized to GAPDH expression as described previously (52).

Statistical analysis

Data from groups were compared using GraphPad Prism, version 8 software (GraphPad Software, Inc), and nonparametric testing was performed by the Mann–Whitney rank sum test for two groups and Kruskal–Wallis two-way ANOVA on ranks for three or more groups.

Data availability

All data in this study are within the manuscript.

Supporting information—This article contains supporting information.

Author contributions—L. L. and M. A. conceptualization; L. L. methodology; L. L. and M. A. validation; L. L. and M. A. formal analysis; L. L. and M. A. investigation; M. A. resources; L. L. and M. A. data curation; L. L. writing–original draft; M. A. writing–review and editing; M. A. supervision; L. L. and M. A. project administration; M. A. funding acquisition.

Conflict of interest—The authors declare that they have no conflicts of interest with the contents of this article.

Abbreviations—The abbreviations used are: APRIL, a proliferation-inducing ligand; BAFF, B-cell–activating factor; BCMA, B-cell maturation antigen; DAPI, 4′,6-diamidino-2-phenylindole; ERK, extracellular signal–regulated kinase; FACS, fluorescence-activated cell sorting; Ig, immunoglobulin; IL, interleukin; Ion, ionomycin; LPS, lipopolysaccharide; MMP, matrix metalloproteinase; MRL/Lpr, MRL/MpJ-Fas^{lpr}/J; PMA, phenylmercuric acetate; SLE, systemic lupus erythematosus; TACI, transmembrane activator, calcium modulator, cyclophilin ligand interactor; TCM, central memory T; TCRβ, T-cell receptor β; TEM, effector memory T; TN, naive T.

References

1. Tsokos, G. C. (2011) Systemic lupus erythematosus. *N. Engl. J. Med.* **365**, 2110–2121
2. Salazar-Camarena, D. C., Ortiz-Lazareno, P., Marin-Rosales, M., Cruz, A., Munoz-Valle, F., Tapia-Llanos, R., Orozco-Barocio, G., Machado-Contreras, R., and Palafox-Sanchez, C. A. (2019) BAFF-R and TACI expression on CD3+ T cells: Interplay among BAFF, APRIL and T helper cytokines profile in systemic lupus erythematosus. *Cytokine* **114**, 115–127
3. Sakai, J., and Akkoyunlu, M. (2017) The role of BAFF system molecules in host response to pathogens. *Clin. Microbiol. Rev.* **30**, 991–1014
4. Hahn, B. H. (2013) Belimumab for systemic lupus erythematosus. *N. Engl. J. Med.* **368**, 1528–1535
5. Minowa, K., Amano, H., Nakano, S., Ando, S., Watanabe, T., Nakiri, Y., Amano, E., Tokano, Y., Morimoto, S., and Takasaki, Y. (2011) Elevated serum level of circulating syndecan-1 (CD138) in active systemic lupus erythematosus. *Autoimmunity* **44**, 357–362
6. Kim, K. J., Kim, J. Y., Baek, I. W., Kim, W. U., and Cho, C. S. (2015) Elevated serum levels of syndecan-1 are associated with renal involvement in patients with systemic lupus erythematosus. *J. Rheumatol.* **42**, 202–209
7. Alexopoulou, A. N., Multhaupt, H. A., and Couchman, J. R. (2007) Syndecans in wound healing, inflammation and vascular biology. *Int. J. Biochem. Cell Biol.* **39**, 505–528
8. Kim, C. W., Goldberger, O. A., Gallo, R. L., and Bernfield, M. (1994) Members of the syndecan family of heparan sulfate proteoglycans are expressed in distinct cell-, tissue-, and development-specific patterns. *Mol. Biol. Cell* **5**, 797–805
9. Theocharis, A. D., Skandalis, S. S., Tzanakakis, G. N., and Karamanos, N. K. (2010) Proteoglycans in health and disease: Novel roles for proteoglycans in malignancy and their pharmacological targeting. *FEBS J.* **277**, 3904–3923
10. Couchman, J. R. (2003) Syndecans: Proteoglycan regulators of cell-surface microdomains? *Nat. Rev. Mol. Cell Biol.* **4**, 926–937
11. Endo, K., Takino, T., Miyamori, H., Kinsen, H., Yoshizaki, T., Furukawa, M., and Sato, H. (2003) Cleavage of syndecan-1 by membrane type matrix metalloproteinase-1 stimulates cell migration. *J. Biol. Chem.* **278**, 40764–40770
12. Manon-Jensen, T., Itoh, Y., and Couchman, J. R. (2010) Proteoglycans in health and disease: The multiple roles of syndecan shedding. *FEBS J.* **277**, 3876–3889
13. Fitzgerald, M. L., Wang, Z., Park, P. W., Murphy, G., and Bernfield, M. (2000) Shedding of syndecan-1 and -4 ectodomains is regulated by multiple signaling pathways and mediated by a TIMP-3-sensitive metalloproteinase. *J. Cell Biol.* **148**, 811–824
14. Palaiologou, M., Delladetsima, I., and Tiniakos, D. (2014) CD138 (syndecan-1) expression in health and disease. *Histol. Histopathol.* **29**, 177–189
15. Elenius, V., Gotte, M., Reizes, O., Elenius, K., and Bernfield, M. (2004) Inhibition by the soluble syndecan-1 ectodomains delays wound repair in mice overexpressing syndecan-1. *J. Biol. Chem.* **279**, 41928–41935
16. Kato, M., Wang, H., Kainulainen, V., Fitzgerald, M. L., Ledbetter, S., Ornitz, D. M., and Bernfield, M. (1998) Physiological degradation converts the soluble syndecan-1 ectodomain from an inhibitor to a potent activator of FGF-2. *Nat. Med.* **4**, 691–697
17. Nikolova, V., Koo, C. Y., Ibrahim, S. A., Wang, Z., Spillmann, D., Dreier, R., Kelsch, R., Fischgrabe, J., Smollich, M., Rossi, L. H., Sibrowski, W., Wulfing, P., Kiesel, L., Yip, G. W., and Gotte, M. (2009) Differential roles for membrane-bound and soluble syndecan-1 (CD138) in breast cancer progression. *Carcinogenesis* **30**, 397–407
18. Purushothaman, A., Chen, L., Yang, Y., and Sanderson, R. D. (2008) Heparanase stimulation of protease expression implicates it as a master regulator of the aggressive tumor phenotype in myeloma. *J. Biol. Chem.* **283**, 32628–32636
19. Purushothaman, A., Uyama, T., Kobayashi, F., Yamada, S., Sugahara, K., Rapraeger, A. C., and Sanderson, R. D. (2010) Heparanase-enhanced shedding of syndecan-1 by myeloma cells promotes endothelial invasion and angiogenesis. *Blood* **115**, 2449–2457
20. Yang, Y., Yaccoby, S., Liu, W., Langford, J. K., Pumphrey, C. Y., Theus, A., Epstein, J., and Sanderson, R. D. (2002) Soluble syndecan-1 promotes growth of myeloma tumors *in vivo*. *Blood* **100**, 610–617
21. Joensuu, H., Anttonen, A., Eriksson, M., Makitaro, R., Alfthan, H., Kinnula, V., and Leppa, S. (2002) Soluble syndecan-1 and serum basic fibroblast growth factor are new prognostic factors in lung cancer. *Cancer Res.* **62**, 5210–5217
22. Kyrtsonis, M. C., Vassilakopoulos, T. P., Siakantaris, M. P., Kokoris, S. I., Gribabis, D. A., Dimopoulou, M. N., Angelopoulou, M. K., and Pangalis, G. A. (2004) Serum syndecan-1, basic fibroblast growth factor and osteoprotegerin in myeloma patients at diagnosis and during the course of the disease. *Eur. J. Haematol.* **72**, 252–258
23. Liu, L., Takeda, K., and Akkoyunlu, M. (2020) Disease stage-specific pathogenicity of CD138 (syndecan 1)-expressing T cells in systemic lupus erythematosus. *Front. Immunol.* **11**, 1569

24. Li, W., Titov, A. A., and Morel, L. (2017) An update on lupus animal models. *Curr. Opin. Rheumatol.* **29**, 434–441
25. Richard, M. L., and Gilkeson, G. (2018) Mouse models of lupus: What they tell us and what they don't. *Lupus Sci. Med.* **5**, e000199
26. Liu, L., Allman, W. R., Coleman, A. S., Takeda, K., Lin, T. L., and Akkoyunlu, M. (2018) Delayed onset of autoreactive antibody production and M2-skewed macrophages contribute to improved survival of TACI deficient MRL-Fas/Lpr mouse. *Sci. Rep.* **8**, 1308
27. Subramanian, S. V., Fitzgerald, M. L., and Bernfield, M. (1997) Regulated shedding of syndecan-1 and -4 ectodomains by thrombin and growth factor receptor activation. *J. Biol. Chem.* **272**, 14713–14720
28. Ding, K., Lopez-Burks, M., Sanchez-Duran, J. A., Korc, M., and Lander, A. D. (2005) Growth factor-induced shedding of syndecan-1 confers glypican-1 dependence on mitogenic responses of cancer cells. *J. Cell Biol.* **171**, 729–738
29. Brule, S., Charnaux, N., Sutton, A., Ledoux, D., Chaigneau, T., Saffar, L., and Gattegno, L. (2006) The shedding of syndecan-4 and syndecan-1 from HeLa cells and human primary macrophages is accelerated by SDF-1/CXCL12 and mediated by the matrix metalloproteinase-9. *Glycobiology* **16**, 488–501
30. Owen, J. L., Iragavarapu-Charyulu, V., Gunja-Smith, Z., Herbert, L. M., Grosso, J. F., and Lopez, D. M. (2003) Up-regulation of matrix metalloproteinase-9 in T lymphocytes of mammary tumor bearers: Role of vascular endothelial growth factor. *J. Immunol.* **171**, 4340–4351
31. Koshikawa, N., Hasegawa, S., Nagashima, Y., Mitsuhashi, K., Tsubota, Y., Miyata, S., Miyagi, Y., Yasumitsu, H., and Miyazaki, K. (1998) Expression of trypsin by epithelial cells of various tissues, leukocytes, and neurons in human and mouse. *Am. J. Pathol.* **153**, 937–944
32. Hargreaves, D. C., Hyman, P. L., Lu, T. T., Ngo, V. N., Bidgol, A., Suzuki, G., Zou, Y. R., Littman, D. R., and Cyster, J. G. (2001) A coordinated change in chemokine responsiveness guides plasma cell movements. *J. Exp. Med.* **194**, 45–56
33. Biajoux, V., Natt, J., Freitas, C., Alouche, N., Sacquin, A., Hemon, P., Gaudin, F., Fazilleau, N., Espeli, M., and Balabanian, K. (2016) Efficient plasma cell differentiation and trafficking require Cxcr4 desensitization. *Cell Rep.* **17**, 193–205
34. Rui, L., Healy, J. I., Blasioli, J., and Goodnow, C. C. (2006) ERK signaling is a molecular switch integrating opposing inputs from B cell receptor and T cell cytokines to control TLR4-driven plasma cell differentiation. *J. Immunol.* **177**, 5337–5346
35. Moreaux, J., Sprynski, A. C., Dillon, S. R., Mahtouk, K., Jourdan, M., Ythier, A., Moine, P., Robert, N., Jourdan, E., Rossi, J. F., and Klein, B. (2009) APRIL and TACI interact with syndecan-1 on the surface of multiple myeloma cells to form an essential survival loop. *Eur. J. Haematol.* **83**, 119–129
36. Ingold, K., Zumsteg, A., Tardivel, A., Huard, B., Steiner, Q. G., Cachero, T. G., Qiang, F., Gorelik, L., Kalled, S. L., Acha-Orbea, H., Rennert, P. D., Tschopp, J., and Schneider, P. (2005) Identification of proteoglycans as the APRIL-specific binding partners. *J. Exp. Med.* **201**, 1375–1383
37. Uslu, K., Coleman, A. S., Allman, W. R., Katsenelson, N., Bram, R. J., Alugupalli, K. R., and Akkoyunlu, M. (2014) Impaired B cell receptor signaling is responsible for reduced TACI expression and function in X-linked immunodeficient mice. *J. Immunol.* **192**, 3582–3595
38. Yasuda, T., Kometani, K., Takahashi, N., Imai, Y., Aiba, Y., and Kurosaki, T. (2011) ERKs induce expression of the transcriptional repressor Blimp-1 and subsequent plasma cell differentiation. *Sci. Signal.* **4**, ra25
39. Schweighoffer, E., and Tybulewicz, V. L. (2018) Signalling for B cell survival. *Curr. Opin. Cell Biol.* **51**, 8–14
40. Mackay, F., and Schneider, P. (2009) Cracking the BAFF code. *Nat. Rev. Immunol.* **9**, 491–502
41. Bossen, C., Cachero, T. G., Tardivel, A., Ingold, K., Willen, L., Dobles, M., Scott, M. L., Maquelin, A., Belnoue, E., Siegrist, C. A., Chevrier, S., Acha-Orbea, H., Leung, H., Mackay, F., Tschopp, J., *et al.* (2008) TACI, unlike BAFF-R, is solely activated by oligomeric BAFF and APRIL to support survival of activated B cells and plasmablasts. *Blood* **111**, 1004–1012
42. Bernfield, M., Gotte, M., Park, P. W., Reizes, O., Fitzgerald, M. L., Lincecum, J., and Zako, M. (1999) Functions of cell surface heparan sulfate proteoglycans. *Annu. Rev. Biochem.* **68**, 729–777
43. McCarron, M. J., Park, P. W., and Fooksman, D. R. (2017) CD138 mediates selection of mature plasma cells by regulating their survival. *Blood* **129**, 2749–2759
44. Seidel, C., Sundan, A., Hjorth, M., Turesson, I., Dahl, I. M., Abildgaard, N., Waage, A., and Borset, M. (2000) Serum syndecan-1: A new independent prognostic marker in multiple myeloma. *Blood* **95**, 388–392
45. Mali, M., Andtfolk, H., Miettinen, H. M., and Jalkanen, M. (1994) Suppression of tumor cell growth by syndecan-1 ectodomain. *J. Biol. Chem.* **269**, 27795–27798
46. Dhodapkar, M. V., Abe, E., Theus, A., Lacy, M., Langford, J. K., Barlogie, B., and Sanderson, R. D. (1998) Syndecan-1 is a multifunctional regulator of myeloma pathobiology: Control of tumor cell survival, growth, and bone cell differentiation. *Blood* **91**, 2679–2688
47. Jung, O., Trapp-Stamborski, V., Purushothaman, A., Jin, H., Wang, H., Sanderson, R. D., and Rapraeger, A. C. (2016) Heparanase-induced shedding of syndecan-1/CD138 in myeloma and endothelial cells activates VEGFR2 and an invasive phenotype: Prevention by novel synstatins. *Oncogenesis* **5**, e202
48. Mahtouk, K., Cremer, F. W., Reme, T., Jourdan, M., Baudard, M., Moreaux, J., Requirand, G., Fiol, G., De Vos, J., Moos, M., Quittet, P., Goldschmidt, H., Rossi, J. F., Hose, D., and Klein, B. (2006) Heparan sulphate proteoglycans are essential for the myeloma cell growth activity of EGF-family ligands in multiple myeloma. *Oncogene* **25**, 7180–7191
49. Bischof, D., Elsawa, S. F., Mantchev, G., Yoon, J., Michels, G. E., Nilson, A., Sutor, S. L., Platt, J. L., Ansell, S. M., von Bulow, G., and Bram, R. J. (2006) Selective activation of TACI by syndecan-2. *Blood* **107**, 3235–3242
50. O'Connor, B. P., Raman, V. S., Erickson, L. D., Cook, W. J., Weaver, L. K., Ahonen, C., Lin, L. L., Mantchev, G. T., Bram, R. J., and Noelle, R. J. (2004) BCMA is essential for the survival of long-lived bone marrow plasma cells. *J. Exp. Med.* **199**, 91–98
51. Schneider, P. (2005) The role of APRIL and BAFF in lymphocyte activation. *Curr. Opin. Immunol.* **17**, 282–289
52. Liu, L., Inouye, K. E., Allman, W. R., Coleman, A. S., Siddiqui, S., Hotamisligil, G. S., and Akkoyunlu, M. (2018) TACI-deficient macrophages protect mice against metaflammation and obesity-induced dysregulation of glucose homeostasis. *Diabetes* **67**, 1589–1603